

MSFR: MATERIAL ISSUES AND THE EFFECT OF CHEMISTRY CONTROL

S. Delpech⁽¹⁾, E. Merle-Lucotte⁽²⁾, T. Auger⁽³⁾, X. Doligez⁽⁴⁾, D. Heuer⁽⁵⁾, G. Picard⁽⁶⁾

(1) Sylvie Delpech – Centre national de la recherche scientifique (*sylvie-delpech@chimie-paristech.fr*)

(2) Elsa Merle-Lucotte – Centre national de la recherche scientifique (*merle@lpsc.in2p3.fr*)

(3) Thierry Auger – Centre national de la recherche scientifique (*thierry.auger@ecp.fr*)

(4) Xavier Doligez – Centre national de la recherche scientifique (*doligez@lpsc.in2p3.fr*)

(5) Daniel Heuer – Centre national de la recherche scientifique (*Daniel.Heuer@lpsc.in2p3.fr*)

(6) Gérard Picard – Centre national de la recherche scientifique (*gerard-picard@chimie-paristech.fr*)

I INTRODUCTION

An innovative molten salt reactor concept, the MSFR (Molten Salt Fast Reactor) is developed by CNRS (France) since 2004. [1,2] Based on the particularity of using a liquid fuel, this concept is derived from the American molten salt reactors (included the demonstrator MSRE) developed in the 1960s. [3-5]

In MSFR, the ORNL (Oak Ridge National Laboratory) MSBR concept has been revisited by removing graphite and BeF₂. The neutron spectrum is fast and the reprocessing rate strongly reduced down to 40 liters per day (compared to 4000l/day in the MSBR concept) to get a positive breeding gain. The reactor is started with ²³³U or with a Pu and minor actinides (MA) mixture from PWR spent fuel. The MA consumption with burn-up demonstrates the burner capability of MSFR. [1,2]

The structural materials retained for MSR container are Ni-based alloys with a low concentration of Cr. The composition of Hastelloy N (Ni-Mo-Cr system) optimized by ORNL researchers is already a good candidate for temperature up to 750°C. The operating temperatures chosen in neutronic calculations of MSFR systems are ranged between 700 and 850°C. For this high temperature domain, the

replacement of Mo by W looks promising from the mechanical properties point of view.

This paper addresses the issue of structural materials considering the mechanical properties at high temperature, the neutronic irradiation damages and the chemical compatibility with the fuel salt.

II. MECHANICAL PROPERTIES

The Oak Ridge program on the molten salt reactor experiment led to the development of the Hastelloy N alloy, essentially a Nickel ternary alloy added with 8wt% of Cr and 12wt% of Mo. [6] The composition of the alloy was optimized for corrosion resistance, irradiation resistance and high temperature mechanical properties. Pure nickel has a good compatibility with fluorides but lacks the required high strength at high temperature.

Molybdenum, which also has a good compatibility with fluorides, was therefore added in solid solution to nickel to provide high temperature creep resistance and hardening.

The composition of Cr was tailored on the one side to maintain a good corrosion resistance in gas atmosphere containing oxygen due to the formation of a protective oxide. On the other side, the content of Cr was limited in order to

suppress voids formation due to the Cr depletion by dissolution in the molten salt.

Helium produced by neutron capture on the isotope ^{58}Ni dominates the issue of the resistance of the material under irradiation. A modified version of Hastelloy N was designed with an improved irradiation resistance due to a fine dispersion of titanium and niobium carbides. These carbides provide coherent interfaces to the nickel matrix which very efficiently traps He atoms.

One can say that within the temperature range envisioned for molten salt reactors at that time (maximum temperature of 700-720°C), there is a first generation structural material that satisfies requested criteria. However, it was also demonstrated that the maximum temperature allowable for this material is of the order of 750°C. Indeed, beyond this threshold, titanium and niobium carbides are dissolved in the nickel matrix. Due to its evolving microstructure, it would therefore be impossible to preserve the material properties required to address the specificity of molten salt reactors at higher temperature.

Replacing molybdenum by tungsten in such alloys could prove beneficial to reach higher in-service temperature from several standpoints. First of all, tungsten diffusion is roughly ten times slower in nickel than molybdenum diffusion [7]. Therefore, there is correspondingly a better creep resistance expected with a Ni-W solid solution than with a Ni-Mo solid solution. This would help to reach higher in-service temperature. Second, a comparison of the ternary phase diagram of Ni-Mo-Cr with Ni-W-Cr shows that there is only one intermetallic phase with a high Cr content. Close to the solubility limit in the low chromium range, there is no embrittling intermetallic in the Ni-W-Cr system. Instead, there is a phase separation between the solid solution and a pure W α -phase (see Figure 1).

The kinetic of precipitation being slow, it allows higher temperature to be used in thermo-mechanical processing for microstructure control with much less susceptibility for intermetallics formation. This can also be used to engineer the

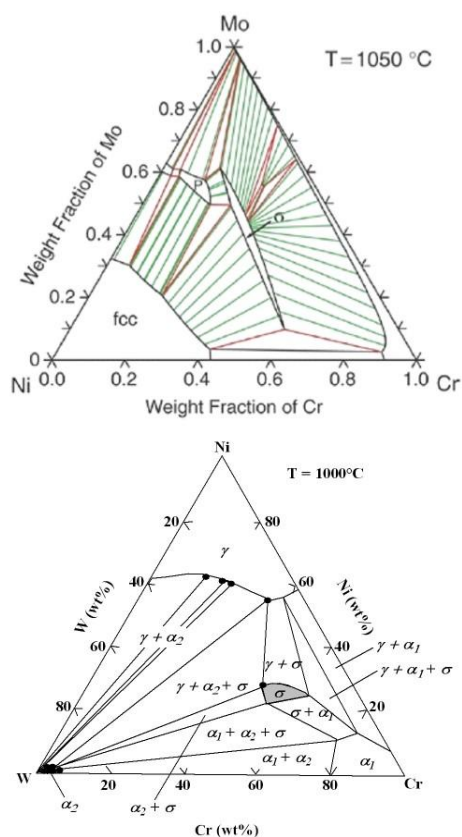


Figure 1: a) Ni-Mo-Cr ternary phase diagram at 1050°C
b) Ni-W-Cr ternary phase diagram at 1000°C

microstructure with tungsten precipitates at grain boundaries. This has been done with success for VHTR materials in the seventies. [8] Having such a microstructure with grain boundaries locked in by tungsten precipitates could be another road to process higher temperature materials for molten salt reactors with outstanding mechanical properties. Indeed, such a microstructure with tungsten precipitates at grain boundaries would be stable up to very high temperature. High temperature grain growth would be reduced as well as grain boundary sliding leading to an increased creep resistance. Solubility limits in this ternary system are not well known but are currently being investigated. Preliminary results show that indeed one can precipitate tungsten in the low Cr range as well in reasonable time allowing for the definition of an industrial material. Therefore, Ni-W-Cr alloys look promising for their use in molten salt at high temperature.

II. NEUTRONIC IRRADIATION DAMAGES

Ni-Mo-Cr alloys were tested under irradiation. The helium formation and diffusion at grain boundaries can be responsible of the metallic alloy embrittlement. The main part of Helium is produced by the action of thermal neutrons on nickel. Niobium and titanium carbides are added to the metallic alloy to trap helium atoms and therefore prevent the alloy embrittlement.

Neutronic calculations have been performed (using MCNP neutron transport code coupled with the lab-made materials evolution code REM) in the case of molten salt reactor operating in a fast spectrum (MSFR) and for Ni-W-Cr alloys which is required for high operation temperature. The neutronic irradiation damages modify the properties of the materials through three effects: the displacements of atoms, the helium production and the transmutation of tungsten to osmium by nuclear reaction. These results obtained for the material damages are presented here for the upper axial reflector [9] which is the most irradiated element in the core, the neutron flux in this reflector being displayed in Figure 2.

III-A- Displacements of atoms

The radiation damages in neutron-irradiated materials depend on many factors (neutron spectrum and flux, irradiation dose) and are expressed in displacements per atom (dpa). That corresponds to the number of times an atom is displaced for a given fluence. The calculations show that the damages are largest in the first two centimeters of the central area (radius 20 cm and thickness 2 cm) of the axial reflector and are quite small, varying from 0.47 dpa/year (for a fuel salt volume of 27 m³) to 1.17 dpa/year (for a fuel salt volume of 12 m³).

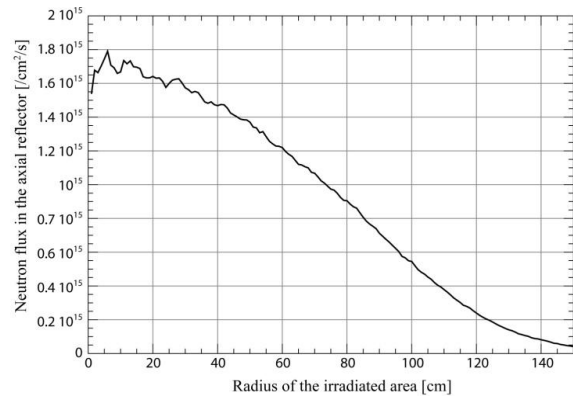


Figure 2: Neutron flux in the axial reflector of the MSFR as a function of the irradiated area considered (zero corresponding to the centre of the core), for a fuel salt volume of 18 m³

III-B- Helium production

The helium concentration in the structural material is directly determined by its production rates through nuclear reactions. Helium production depends on the boron and nickel amounts in the alloy. It is produced by two nuclear reactions: $^{10}\text{B}(n,\alpha)^7\text{Li}$ and $^{58}\text{Ni}(n,\alpha)^{55}\text{Fe}$. As shown in Figure 3 and as it was previously observed in thermal spectrum (MSRE), the main part of helium is produced by the nickel transmutation.

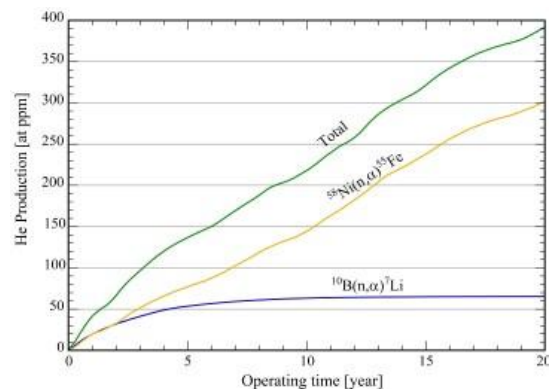


Figure 3: Production of He in the most irradiated part of the axial reflector (radius 20 cm and thickness 2 cm) of MSFR system with a volume core of 18 m³.

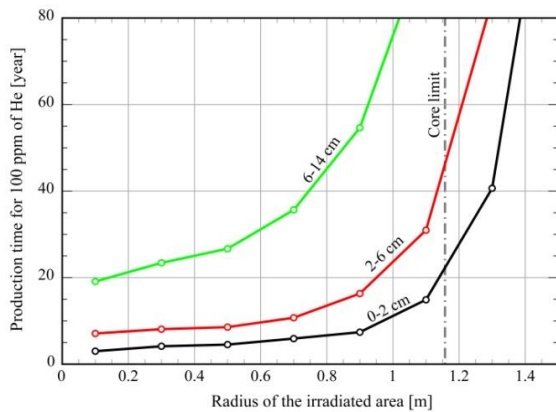


Figure 4: Operation time necessary to produce 100 ppm of He in different depths of the axial reflector as a function of the irradiated area considered (zero corresponding to the centre of the core), for a fuel salt volume of 18 m³

Moreover, the content of boron can be strongly reduced in the structural material. The largest acceptable amount of helium in the material is not known and the diffusion of helium in Ni-W-Cr alloys has not been yet determined. If we assume that the acceptable limit is equal to a production of 100 ppm of Helium, [15] the equivalent operation time to reach this value are displayed in Figure 4. These operation times, larger than 170 years for the deeper zones of this reflector (from 14 to 30 cm), are not represented. As a conclusion, regular replacements of the most irradiated area of the upper axial reflector have to be planned, but it concerns only its first 15 centimeters.

III-C- Osmium production

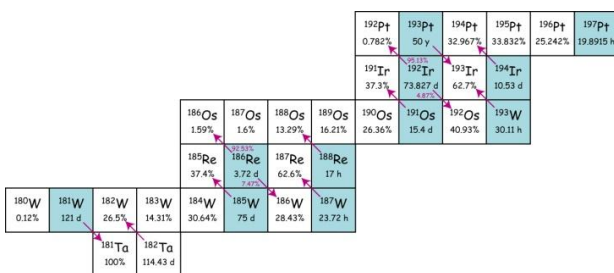


Figure 5: Transmutation cycle of Tungsten, Rhenium and Osmium, due to the neutronic captures; the blue boxes represent the unstable nuclei that decay through the purple arrows

Nuclear reactions lead to tungsten transmutation into rhenium and osmium, as shown

in Figure 5. The proportion of transmutation has been calculated and is given in Figure 6 with a neutron flux lower than $1.6 \cdot 10^{15}$ neutrons/cm²/s in the most irradiated part of the structural material (see Figure 2), to be compared to the neutron flux in the core itself which is around 5 times higher.

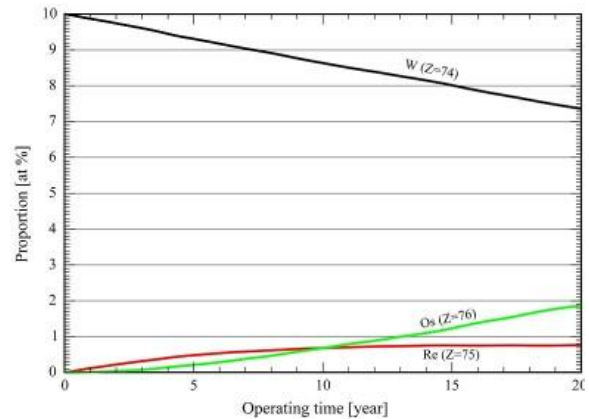


Figure 6: Composition evolution of alloy in W, Os and Rh in the most irradiated part of the axial reflector (central area of radius 20 cm and thickness 2 cm) as a function of operating time, with a fuel salt volume of 18 m³

Considering that a loss of less than 1at% of tungsten is acceptable, the most irradiated part of the upper reflector has thus to be changed every 5 to 10 years.

Table 1 gathers the results obtained for the different irradiation damages as a function of fuel salt volume, in terms of reactor operation times necessary to produce these damages. The damages are inversely proportional to the fuel salt volume favoring the larger MSFR configurations.

Fuel salt Volume (m ³)	Time (year) (100 dpa)	Time (year) (100 ppm He)	Time (year) (-1at% of W)
12	85	2.2	4.7
18	133	3.2	7.3
27	211	5.5	10.9

Table 1: Reactor operation time necessary to reach a given irradiation damages in the most irradiated part of the axial reflector (central area of radius 20 cm and thickness 2 cm), as a function of the fuel salt volume.

The feasibility of using reflectors made of metallic alloy has been demonstrated from a

neutronic point of view. The irradiation damages have been evaluated and the replacement of a part of the axial reflector every five years for example is not a drawback.

IV. CHEMICAL BEHAVIOUR

The chemical behavior of a metallic element or alloy strongly depends on its environment. In the case of fuel salt, the chemical properties of the molten salt will define the chemical behavior of the structural materials. The presence of some fission products can also be responsible of chemical reactions but the main chemical corrosion can be controlled by the control of salt properties.

In Ni-Mo-Cr or Ni-W-Cr alloys, the more easily oxidizable element is Cr because its redox potential is very low. Therefore the main corrosion is due to the dissolution of chromium.

IV-A- Salt properties

The fluoride molten salt is characterized by its redox potential and its oxo-acidity (concentration of free oxide ions in the molten salt). Using thermochemical data, equilibrium diagrams [10] can be calculated giving the stability ranges of different elements in a given molten salt at a given temperature. Such a diagram has been calculated for chromium (Figure 7). This diagram shows the stability of the different chromium-based compounds in their different oxidation states which can be present in the molten salt as a function of the potential and of the oxo-acidity. The oxo-acidity is given by the activity of oxide in the molten salt. For thermochemical calculations, the oxo-acidity is calculated introducing the activity of Li_2O . The relation between the activity of Li_2O and the oxide activity can be determined experimentally and depends on the nature of the molten salt.

The Figure 7 shows that Cr is oxidized for potential higher than -3.5V when the $\text{pa}(\text{Li}_2\text{O})$ is ranging between 12 and 25. When the acidity decreases (low values of $\text{pa}(\text{Li}_2\text{O})$) the oxidation of Cr occurs at lower potentials values (between -4.5 and -3.5V).

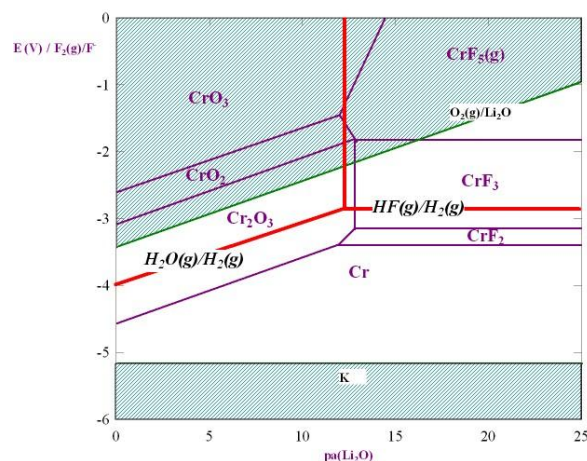


Figure 7: Potential-acidity diagram calculated for Cr in fluoride media at 700°C calculated for activities equal to 1.

Cr can be oxidized to CrF_2 solubilized in the molten salt. Depending on the oxo-acidity of the melt, Cr can also be oxidized to Cr_2O_3 . If the oxo-acidity (given in $\text{pa}(\text{Li}_2\text{O}) = -\log [a(\text{Li}_2\text{O})]$) of the melt is lower than 13, the oxidation of Cr leads to the formation of the oxide Cr_2O_3 which is known to be protective against corrosion under oxygen atmosphere. However, the high purification of fluoride molten salt contributes to reach very low amounts of oxide (high values of $\text{pa}(\text{Li}_2\text{O})$) and in these conditions the chromium oxide is not stable and its oxidation leads to the formation of soluble compounds such as CrF_2 .

On the other hand, the high purification of melts against oxide ions is required to prevent the precipitation of solid oxides (such as UO_2 or ThO_2) in the fuel salt. To overcome this dilemma, addition of ZrF_4 was recommended to control the oxide concentration (by precipitation of ZrO_2 insoluble in fluoride molten salt) and the MSRE fuel salt was constituted of 5mol% of ZrF_4 .

IV-B- Potential control

The control of redox potential of the fuel salt is the best way to prevent the oxidation of chromium. It is possible to control the redox potential by using a redox “buffer” constituted by the two oxidation states of uranium, UF_4 and UF_3 . The fuel potential is given by the following Nernst relation:

$$E(V) = E^\circ + (2.3RT/F) \log ([\text{UF}_4]/[\text{UF}_3]) \quad (1)$$

where E° is the standard potential of the redox system (V), R the ideal gas constant (J/mol/K), T the temperature (K), F the Faraday constant (96500C), $[UF_4]$ and $[UF_3]$ respectively the concentrations of UF_4 and UF_3 in the fuel salt.

This ratio can vary from 10 to 100. The lowest limit is given by the solubility of UF_3 and the largest limit by the higher potential acceptable for chromium corrosion.

The dissolution of chromium can be described by the following reaction:



The variation of the constant K , which characterizes this equilibrium, with the temperature was experimentally established by Baes [11]. Considering the activity of chromium in the alloy (equal to 0.083 [12]), the concentration of CrF_2 can be calculated for various ratios $[UF_4]/[UF_3]$ as a function of temperature (Figure 8).

Figure 8 shows a large difference of the concentration of CrF_2 as a function of temperature. That explains the mass transfer observed experimentally by the ORNL [14] in the convective loops between the hot and the cold parts of the loop. A dissolution of chromium is observed in the hot part of the loop and deposits of metallic chromium are observed in the cold part of the loop. The redox potential applied by the ratio of UF_4/UF_3 is not sufficiently low to prevent the oxidation of metallic chromium in the temperature range of the fuel.

Nevertheless, experimental corrosion tests in molten salt loops have shown that the deposits of chromium were very homogeneous without any dendrites and no clogged pipes were observed.

IV-C- Evolution of fuel potential with operation time

It was demonstrated that a redox potential control of the fuel salt is necessary to limit the corrosion of structural materials. However the potential of the fuel salt increases with the

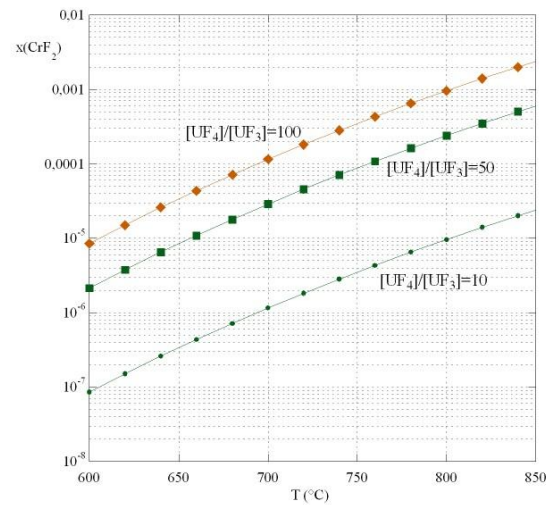
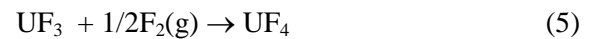


Figure 8: Variation of the concentration of CrF_2 in the fuel salt as a function of temperature for various ratios $[UF_4]/[UF_3]$

operation time due to the fission reaction. The fissile element in the liquid fuel is uranium. As it was previously described, uranium is dissolved in the fuel under two chemical states, UF_4 and UF_3 . When the fission reaction occurs, the fission products are essentially lanthanides (LnF_3) (at an oxidation state III) and gaseous products or noble metals (M) (at an oxidation state 0). The impact of the fission reactions on the chemistry can be schematized by:



When the fission occurs on UF_4 , it leads to the formation of gaseous fluorine $F_2(g)$. Fluorine gas is an oxidizing element which contributes to increase the redox potential of the fuel salt by the following way:



The consumption of UF_3 as in (5) leads to an increase of the redox potential of the fuel salt according to the relation (1). To decrease the potential during the operation time, a reducing agent is added in the fuel salt: metallic Be in the case of MSRE system and metallic Th in the MSFR concept.

The redox potential has to be well controlled. Indeed, a very low potential value is not desired because in this case, the tritium produced by fission reaction is under gaseous state (TH or T₂) and a large part will diffuse through the structural material in the heat exchangers. When the tritium is under TF state, it is totally extracted by helium bubbling.

IV-D- Corrosion by fission products

Some fission products are corrosive. A small hydrogen production is observed during MSFR operation. The combination of hydrogen with fluorine or oxygen can occur. The chemical form of hydrogen depends both on oxo-acidity and redox potential of the fuel salt. For example, HF and H₂O which can be reduced to H₂(g) by reacting with chromium. Tellurium is also a corrosive product and it is known to be responsible of an intergranular corrosion of Hastelloy N. [13] Tellurium is in the periodic classification in the same column than O or S. Therefore Te, in its metallic state, is an oxidizing agent which can react with metallic chromium. To prevent the oxidation of Cr with Te, it is necessary to control the redox potential of the fuel salt as well as to produce tellurium in its reduced state.

IV-E- Experimental corrosion tests

The large feed-back of MSRE experience and tests in convection loops performed by the ORNL have demonstrated the high resistance against corrosion of Hastelloy N in fuel salt. The corrosion rate is lower than 3µm/year. The Table 2 gives some results obtained in convection loops [14] in LiF-BeF₂-UF₄ or LiF-BeF₂-ThF₄-UF₄ molten salts.

IV. CONCLUSION

A wide range of problems lies ahead in the design of high temperature materials for molten salt reactors. The Ni-W-Cr system looks promising. First results show that such materials have the required properties, especially in terms of compatibility with molten salts and mechanical properties. Their metallurgy and in-service properties need to be investigated in

Alloy	T(°C)	Convection	Corrosion Rate (µm/year)
LiF-BeF ₂ -UF ₄			
Hastelloy N modified	676	Natural	0.5
	700		0.9
Hastelloy N Standard	660		1
LiF-BeF ₂ -ThF ₄ -UF ₄			
Hastelloy N modified	700		0.4
	704-566	Forced 3 to 6 m/s	3
	dT=55		1.5
Hastelloy N Standard	700	Natural	0.5

Table 2: Results of corrosion tests in convection loops obtained by the ORNL

further details regarding irradiation resistance and industrialization.

These damages are dominated by helium production due to the (n, α) reaction on ⁵⁸Ni. One solution may consist in regularly changing only the first 15 centimeters of the reflectors.

The irradiation damages are logically inversely proportional to the fuel salt volume of the reactor, the smallest volumes (lower than around 15 m³) only being really disfavored due to a high Helium production.

The chemical corrosion can be controlled by a redox buffer which controls the potential of fuel salt. The redox buffer considered is the redox system UF₄/UF₃. The potential has to be measured on line in the reactor core because the potential increases with operation time due to the fission reaction. Addition of a reducing agent leads to a decrease of the fuel salt potential. The use of an acido-basic buffer to control also the oxo-acidity of the molten salt could stabilize the chromium oxide in the alloy and contribute to the formation of a protecting layer at the alloy surface. The experimental feedback from the ORNL has demonstrated the high corrosion resistance of Ni-based alloys in fluoride molten salts.

Acknowledgements

The authors wish to thank PACEN (Programme Aval du Cycle Electronucleaire) of the *Centre National de la Recherche Scientifique* (CNRS) for financial support of these studies.

References

1. Merle-Lucotte, E., D. Heuer, *et al.*, Proc. of the International Conference on the Physics of Reactors PHYSOR 2008, Interlaken, Switzerland, (2008)
2. Delpech, S., E. Merle-Lucotte, *et al.*, *J. of Fluorine Chem.*, 130, 1, 11, (2009)
3. Haubenreich, P. N., J.R. Engel, *Nuclear Appl. & Tech.*, 8, 118, (1970)
4. Grimes, W.R., "Molten salt reactor chemistry", *Nuclear Appl. & Tech.*, 8, 137, (1970)
5. Bettis, E.S., R.C. Robertson, *Nuclear Appl. & Tech.*, 8, 190, (1970)
6. Mc Coy, H.E., *et al.*, *Nuclear Appl. & Tech.*, 8, 156, (1970)
7. Tiernay, T.C., N.J. Grant, *Metallurgical transactions A*, 13A, 1827, (1982)
8. Tanaka, R., T.K. Ondo, *Nuclear Technology*, 66, July (1984) 75
9. Merle-Lucotte, E., D. Heuer, *et al.*, Proc. Of Advanced in Nuclear Fuel Management IV (ANFM 2009), USA, (2009)
10. Rouquette-Sanchez, S., G. Picard, *J. of Electroanal. Chem.*, 572, 173, (2004)
11. Baes, C.F., Proc. of Nuclear Fuel, Conf. 690801, (1969)
12. Grimes, W.R., ORNL report 3708, 238, (1964)
13. Mc Coy, H.E., ORNL report 4812, 201, (1972)
14. Koger, J.W., ORNL report 4832, 124, (1972)
15. Angeliu, T.M., *et al.*, *J. of Nuclear Mat.*, 366(2007)223